

Susceptibility and Dzyaloshinskii-Moriya interaction in the Haldane gap compound NENP

Hai Huang* and Ian Affleck†

Physics Department, Boston University, 590 Commonwealth Ave., Boston, MA02215

Department of Physics and Astronomy, University of British Columbia, Vancouver, BC, Canada, V6T 1Z1

(Dated: January 28, 2020)

The Haldane gap material NENP exhibits anomalies in its Knight shift, far infrared absorption and field-dependent gaps, which have been explained using the staggered g -tensor that occurs due to the low crystal symmetry. We point out that the low-temperature susceptibility is also anomalous and that a consistent interpretation of all data may require consideration of the Dzyaloshinskii-Moriya interaction.

I. INTRODUCTION

$\text{Ni}(\text{C}_2\text{H}_8\text{N}_2)_2\text{NO}_2(\text{ClO}_4)$ (NENP), is one of the best-studied quasi-one-dimensional antiferromagnets which exhibits a “Haldane gap” in its excitation spectrum since the atomic spins have $S=1$. The inter-chain coupling, J' , is estimated to be only $.0004J$, where $J \approx 48K$ is the intra-chain coupling and the disordered phase appears to persist down to zero temperature. Ignoring inter-chain couplings, the standard Hamiltonian for this system consists of Heisenberg exchange plus crystal field terms:

$$H = \sum_j \{J\vec{S}_j \cdot \vec{S}_{j+1} + E^z(S_j^z)^2 + E^x[(S_j^x)^2 - (S_j^y)^2]\}. \quad (1.1)$$

The crystal field interactions split the triplet magnon excitation into 3 separate modes at energies $13.6K$, $15.7K$ and $29K$.¹

However, various anomalies appear in the finite field behavior of NENP. The low temperature susceptibility is much larger than expected from the measured gap anisotropy.² The gap does not close at the Ising transition predicted to occur at a finite critical field.³ At low T the Knight shift (local magnetic field at a nucleus) is much larger than expected.⁴ Production of a single magnon by far infrared absorption is observed even though this is expected to produce only zero wave-vector excitations and a single magnon has wave-vector near π .³

Chiba et al.⁴ pointed out that the Knight shift anomaly can be explained by taking into account the staggered part of the gyromagnetic tensor. They observed that the local crystal structure near a magnetic Ni ion has principal axes which are rotated from the global crystal axes and that the local principal axes take two different orientations for even and odd sites along a chain. The g -tensor and also the crystal field Hamiltonian are expected to align with the local crystal symmetry. This implies that the g -tensor has a staggered component so that an applied uniform magnetic field leads to a small effective staggered field in addition to the uniform one. Because an antiferromagnet responds much more strongly, at low T , to a staggered field than to a uniform one, this leads to large effects at low T . By considering the direction of the staggered field, this theory is successful at explaining the various satellites of the proton Knight shift associated with the various inequivalent H-atoms in the unit cell.

Mitra and Halperin⁵ observed that this staggered field also provides a natural explanation for the field-dependence of the gaps. Since this staggered field is perpendicular to the uniform field it breaks the Z_2 symmetry that would otherwise be present and eliminates the finite field Ising transition. Using a mean field type approximation they attempted to fit the field-dependent gaps by the estimated staggered g -tensor.⁴ Furthermore, because the field is staggered it halves the unit cell making wave-vectors 0 and π equivalent thus explaining the far infrared adsorption anomaly.

So far, no explanation has been offered, as far as we know, for the anomalously large low T susceptibility. Here we observe that the staggered field also provides a natural explanation for this since the measured susceptibility then becomes a sum of uniform and staggered susceptibilities and the latter becomes quite large (but remains finite) at low T . However, we find that it is not possible to consistently fit the susceptibility data in terms of a staggered g -tensor alone.

We also observe that another important effect has been left out of previous explanations of these anomalies. This is the Dzyaloshinskii-Moriya (DM) antisymmetric exchange interaction^{6,7},

$$H_{DM} = \sum_j \vec{D}_j \cdot (\vec{S}_j \times \vec{S}_{j+1}). \quad (1.2)$$

The low crystal symmetry of NENP permits this interaction as well as the staggered g -tensor. A convenient way of treating a DM interaction is to remove it by a gauge transformation. It is possible to exactly eliminate it in favor of

a small symmetric exchange interaction and a small perturbation to the crystal field Hamiltonian which just slightly change the magnon energies. However, the combination of a DM interaction and a magnetic field is less benign. The gauge transformation transforms the uniform field into a combination of uniform, slowly rotating uniform and staggered effective fields. Thus the effective staggered field has two sources which are potentially of the same order of magnitude.

We calculate the susceptibility including the staggered g -tensor and DM interaction using a Ginzburg-Landau (GL) mean field approach.⁸ We also do the calculation using a type of fermionic mean field theory.⁹ Either approach allows quite good fitting of the susceptibility data at low T . A reliable determination of these parameters will probably await accurate numerical results on one-dimensional chains and more accurate experiments. It is possible that still other effects which we continue to ignore such as the staggered crystal field interaction and inter-chain couplings are important. Nonetheless, we expect that our basic conclusion that the DM interaction and staggered g -tensor are of roughly equal importance in explaining these anomalies will remain true.

In the next section we review the crystal symmetry of NENP. Using this plus high- T susceptibility measurements we estimate the uniform and staggered g -tensor. We also derive the most general form of the DM interaction allowed by symmetry. We then go on to discuss the low- T susceptibilities of GL and fermion models in Sec. III. In Sec. IV we comment on other types of experimental data and other theoretical approaches.

II. g -TENSOR AND DZYALOSHINSKII-MORIYA INTERACTION IN NENP

The ethylene-diamine molecule surrounding each magnetic Ni atom in NENP has an approximate orthorhombic symmetry with principal axes rotated relative to those defining the crystal space group. It is convenient to describe this rotation in two stages. Labeling the space group axes (a, b, c) in the conventional way we first introduce a rotation matrix \mathcal{R}_z which rotates by 58° about the b -axis. This defines a co-ordinate system which we label (x, y, z) . (The chain axis, b is identified with z .) The components of the spin operators in this co-ordinate system (S^a) are related to those in the crystallographic system ($S^{a'}$) by:

$$\vec{S} = \mathcal{R}_z \vec{S}'. \quad (2.1)$$

where \mathcal{R}_z is a rotation about the z -axis by $(-\phi)$ ($\phi \approx 58^\circ$):

$$\mathcal{R}_z = \begin{pmatrix} \cos \phi & \sin \phi & 0 \\ -\sin \phi & \cos \phi & 0 \\ 0 & 0 & 1 \end{pmatrix}, \quad (2.2)$$

A further rotation by $\pm\theta$ ($\theta \approx 10^\circ$) about the y -axis, \mathcal{R}_y^\pm , depending on sites:

$$\mathcal{R}_y^\pm = \begin{pmatrix} \cos \theta & 0 & \pm \sin \theta \\ 0 & 1 & 0 \\ \mp \sin \theta & 0 & \cos \theta \end{pmatrix}. \quad (2.3)$$

defines the local symmetry axes around a Ni site, (ξ, ζ, η) . The $+$ or $-$ sign occurs for even or odd sites along a Ni chain. (See Fig. 1.) We label the corresponding spin components \vec{S}'' ,

$$\vec{S}'' = \mathcal{R}_y^\pm \vec{S}. \quad (2.4)$$

The ordinary exchange interaction in NENP is generally assumed to be of the Heisenberg form

$$H_{ex} = J \sum_j \vec{S}_j \cdot \vec{S}_{j+1}. \quad (2.5)$$

However, there is an important symmetry breaking in the crystal field Hamiltonian. This is expected to be diagonal in the \vec{S}'' co-ordinate system, as in Eq. (1.1),

$$H_{CF} = \sum_j \{E^z (S_j^{z''})^2 + E^x [(S_j^{x''})^2 - (S_j^{y''})^2]\}. \quad (2.6)$$

Transforming to the \vec{S} coordinate system, the crystal field Hamiltonian has a diagonal uniform part and a small off-diagonal staggered part. We will assume that the staggered part can be ignored in what follows. The uniform diagonal part could then be fit to the observed magnon gaps. This implies that $E^z \gg E^x > 0$.

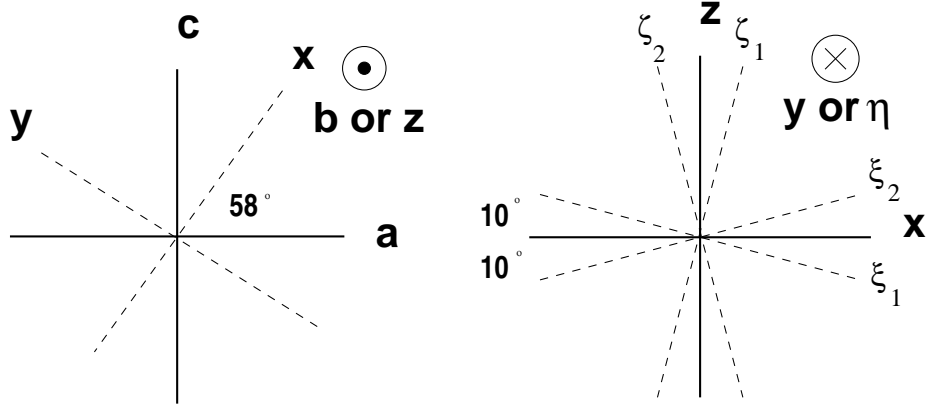


FIG. 1: An illustration of the three co-ordinate systems. 1 and 2 refer to the even and odd sites.

Another important source of anisotropy, when a magnetic field is applied, is the Landé g -tensor, \mathbf{g} . The Zeeman term in the Hamiltonian is written:

$$H_Z = \mu_B \sum_j \vec{h} \cdot \mathbf{g}_j \vec{S}_j. \quad (2.7)$$

The g -tensor is assumed to be diagonal in the (ξ, ζ, η) basis:

$$\mathbf{g}_{(\xi, \eta, \zeta)} = \begin{pmatrix} g_\xi & 0 & 0 \\ 0 & g_\eta & 0 \\ 0 & 0 & g_\zeta \end{pmatrix}. \quad (2.8)$$

The uniform and staggered g -tensors in the (x, y, z) co-ordinate system are given by:

$$\begin{aligned} \mathbf{g}_{(x, y, z)} &= \mathbf{g}^u + \mathbf{g}^s \\ &= (\mathcal{R}_y^\pm) \mathbf{g}_{(\xi, \eta, \zeta)} (\mathcal{R}_y^\pm)^{-1}, \end{aligned} \quad (2.9)$$

where

$$\mathbf{g}^u = \begin{pmatrix} g_x & 0 & 0 \\ 0 & g_y & 0 \\ 0 & 0 & g_z \end{pmatrix} = \begin{pmatrix} g_\xi \cos \theta^2 + g_\zeta \sin \theta^2 & 0 & 0 \\ 0 & g_\eta & 0 \\ 0 & 0 & g_\xi \sin \theta^2 + g_\zeta \cos \theta^2 \end{pmatrix} \quad (2.10)$$

and

$$\mathbf{g}^s = \begin{pmatrix} 0 & 0 & (g_\xi - g_\zeta) \sin \theta \cos \theta \\ 0 & 0 & 0 \\ (g_\xi - g_\zeta) \sin \theta \cos \theta & 0 & 0 \end{pmatrix}. \quad (2.11)$$

The gyromagnetic tensor in the crystallographic coordinate system (a, b, c) can be written as

$$\mathbf{g}_{(a, b, c)} = (\mathcal{R}_z \mathcal{R}_y^\pm) \mathbf{g}_{(\xi, \eta, \zeta)} (\mathcal{R}_z \mathcal{R}_y^\pm)^{-1}. \quad (2.12)$$

A. Dzyaloshinskii-Moriya interaction

As discussed by Dzyaloshinskii⁶ and Moriya⁷, an additional exchange interaction term can appear in the Hamiltonian which is anti-symmetric under interchanging the two sites, the DM interaction

$$H_{DM} = \sum_j \vec{D}_j \cdot (\vec{S}_j \times \vec{S}_{j+1}). \quad (2.13)$$

The possible values of the DM vectors \vec{D}_j can be limited by considering crystal symmetries of NENP, which at low temperatures are given by the space group $Pn2_1a$ ^{5,10}. First, the compound is invariant under a translation along the

\hat{b} (or \hat{z}) by two sites. This means the DM vectors are the same among the even (or odd) links. Second, the crystal structure is invariant under the combined operation of one site translation along the chain (\hat{b}) direction and a 180° rotation around \hat{b} . The operation acts as $S_j^{a,c} \rightarrow -S_{j+1}^{a,c}$, $S_j^b \rightarrow S_{j+1}^b$. This implies that $D_{a,j}$ and $D_{c,j}$ are staggered, $\propto (-1)^j$ while $D_{b,j}$ is uniform. The other symmetry operations relate sites in one chain to sites in the others, so there are no further restrictions on the intra-chain DM vectors.

A nearest neighbor DM interaction in one dimension can always be eliminated by a redefinition of the spin operators which varies from site to site (i.e. a gauge transformation). Let us suppose that the symmetric exchange interaction is $SO(3)$ invariant. Then, choosing co-ordinates so that $\vec{D} \propto \hat{z}$, we may write the combined symmetric and anti-symmetric exchange interactions as:

$$H_{ex} = \sum_j \{ [(J + iD_j)S_j^+ S_{j+1}^- + h.c.] + JS_j^z S_{j+1}^z \} \quad (2.14)$$

We may always transform this into a purely parity-symmetric exchange interaction:

$$H_{ex} = \sum_j [\sqrt{J^2 + D^2} (S_j^x S_{j+1}^x + S_j^y S_{j+1}^y) + JS_j^z S_{j+1}^z], \quad (2.15)$$

by a gauge transformation:

$$S_j^- \rightarrow S_j^- e^{i\alpha_j}. \quad (2.16)$$

When $D_j = (-1)^j D$, the required gauge transformation simply alternates from site to site:

$$\alpha_j = (-1)^j (1/2) \tan^{-1}(D/J). \quad (2.17)$$

On the other hand, for a uniform $D_j = D$,

$$\alpha_j = \alpha \cdot j, \quad (2.18)$$

where

$$\alpha = \tan^{-1}(D/J). \quad (2.19)$$

This gauge transformation introduces a small xxz anisotropy into the symmetric exchange interaction. Its effects on the crystal field Hamiltonian must also be considered. If we write this, in general, as:

$$H_{CF} = \sum_{j,a,b} S_j^a E_j^{ab} S_j^b, \quad (2.20)$$

then the effect of the gauge transformation is:

$$E_j \rightarrow \mathcal{R}(\alpha_j) E_j \mathcal{R}^{-1}(\alpha_j), \quad (2.21)$$

where $\mathcal{R}(\alpha_j)$ is the rotation matrix which effects the gauge transformation of Eq. (2.16):

$$\mathcal{R}(\alpha_j) = \begin{pmatrix} \cos \alpha_j & \sin \alpha_j & 0 \\ -\sin \alpha_j & \cos \alpha_j & 0 \\ 0 & 0 & 1 \end{pmatrix}. \quad (2.22)$$

Thus the principal axes of the crystal field Hamiltonian are rotated from site to site while the eigenvalues remain the same. For an alternating DM interaction, this is an alternating rotation which would introduce an alternating term in the crystal field Hamiltonian. As discussed above, such a term is expected to already be present, before the gauge transformation. For a uniform DM interaction, the transformed E -tensor in the crystal field Hamiltonian rotates steadily along the chain. We will assume these small effects can be ignored.

The combination of a DM interaction and an applied field leads to more important effects. Upon performing the gauge transformation, the g -tensor at site j is transformed as:

$$g_j \rightarrow g_j \mathcal{R}^{-1}(\alpha_j). \quad (2.23)$$

In the case of a staggered DM interaction, this leads to an alternating term in the g -tensor even if it was not present before, thus adding to the effective staggered field. A uniform DM interaction leads to a rotating effective magnetic

field. Both staggered and uniform DM interactions can be readily treated using field theory methods. They appear to be approximately as important as the staggered field in explaining the various anomalies mentioned in Sec. I. We show that it is possible to fit the susceptibility data quite well by taking into account the staggered and uniform DM interactions.

Since the DM interaction contributes the same order of magnitude to the effective staggered field as the staggered gyromagnetic tensor^{11,12}, we have to combine them together. For small \mathbf{g}^s and $(\frac{D}{J})$, and an arbitrary direction for the staggered DM vector $\vec{D}^s = (D_x, D_y, 0)$, the staggered field can be approximated as

$$\vec{h}^s \approx \mathbf{g}^s \vec{h} + \left(\frac{1}{2J}\right) \vec{D}^s \times \mathbf{g}^u \vec{h} \equiv \mathbf{A} \vec{h}, \quad (2.24)$$

which is just the sum of two contributions^{11,12}. Here we have introduced another matrix \mathbf{A} relating the total effective staggered field, \vec{h}^s to the original laboratory field \vec{h} . Note that $|\mathbf{A}| \ll 1$.

Thus after making the gauge transformation and discarding terms which we expect to be unimportant, the Hamiltonian can be written, in the (x, y, z) (\vec{S}) co-ordinate system:

$$H = \sum_j \{ J \vec{S}_j \cdot \vec{S}_{j+1} + E^z (S_j^z)^2 + E^x [(S_j^x)^2 - (S_j^y)^2] - \mu_B \vec{h} \cdot [\mathbf{g}^u \mathcal{R}(\alpha \cdot j)] \vec{S}_j - (-1)^j \mu_B \vec{h}^s \cdot \mathcal{R}(\alpha \cdot j) \vec{S}_j \}, \quad (2.25)$$

where $\mathcal{R}(\alpha \cdot j)$ is defined in Eqs. (2.18) and (2.22). The values of $J \approx 44K$ and $E^z \approx 8K$ have been determined from fitting the magnon gaps to numerical simulations.^{13,14} $E^x \approx 0.4K$ is extracted by the best fit of experimental data to the six-spin-ring model calculation.³

III. SUSCEPTIBILITY

A. Mean Field Results

In the large- s approximation, the Heisenberg spin chain is equivalent to a field theory, the O(3) non-linear σ -model (see, e.g., Ref. 15 and Ref. 16). The Hamiltonian of this model is given by

$$H = \left(\frac{v}{2}\right) \int dz \left[g \vec{l}^2 + \frac{1}{g} \left(\frac{\partial \vec{\phi}}{\partial z}\right)^2 \right] \quad (\vec{\phi}^2 = 1) \quad , \quad (3.1)$$

where

$$\vec{l} = \frac{1}{vg} \vec{\phi} \times \frac{\partial \vec{\phi}}{\partial t}. \quad (3.2)$$

The coupling constant g and the magnon velocity take the values, at $s \rightarrow \infty$,

$$g = \frac{2}{s}, \quad v = 2J. \quad (3.3)$$

The original spin operators are expressed in terms of the field $\vec{\phi}$ and the spin density, \vec{l} as

$$\vec{S}_j \approx (-1)^j s \vec{\phi}_j + \vec{l}_j. \quad (3.4)$$

If we relax the constraint of O(3) non-linear σ -model and add a repulsive ϕ^4 interaction, which is treated perturbatively, a much simpler theory can be obtained. Including anisotropic terms, we then phenomenologically model the low-lying excitations via the following bosonic quantum field theory^{2,17}, which we refer to as the Ginzburg-Landau model (GL model):

$$H = \int dz \left\{ \sum_i \left[\frac{v}{2} \Pi_i^2 + \frac{v}{2} \left(\frac{\partial \phi_i}{\partial z}\right)^2 + \frac{\Delta_i^2}{2v} \phi_i^2 \right] - \mu_B \sum_{iklmn} h_i \mathbf{g}_{ik}^u \mathcal{R}_{kl}(\alpha \cdot z) \epsilon_{lmn} \phi_m \Pi_n - \mu_B \sum_{ik} h_i^s \mathcal{R}_{ik}(\alpha \cdot z) \rho_k \phi_k + \lambda \vec{\phi}^4 \right\}. \quad (3.5)$$

Here ϵ_{ijk} is the anti-symmetric tensor with $\epsilon_{123} = 1$. We assume the gaps, normalization factors and velocity are:

$$\begin{aligned} \Delta_x &= 15.7K, \quad \Delta_y = 13.6K, \quad \Delta_z = 29K; \\ \rho_x &= \rho_y = 1.08, \quad \rho_z = 1.2; \quad v = 120K; \quad \lambda = 3.7K. \end{aligned} \quad (3.6)$$

(We use units where the spacing between neighboring Ni ions along the chains is 1.) The gaps are from neutron scattering experiments²³ and normalization factors and velocity are from numerical simulations.¹³

Tsvelik proposed a fermionic field theory model⁹ for NENP. We can easily include uniform DM interaction into this model. But there is some problem for staggered effective field (including staggered g -tensor and staggered DM interaction). The staggered components of the spin operators have a very complicated representation as the product of three Ising order (and disorder) parameter fields. Consequently, there appears to be no simple method for treating a staggered field in this model. If only uniform DM interaction is taken into account, the Hamiltonian can be modified as

$$H = \int dz \left[\sum_k (i\bar{\chi}_k \gamma_1 \partial_z \chi_k + \Delta_k \bar{\chi}_k \chi_k) - \mu_B \sum_{klmnp} i h_k \mathbf{g}_{kl}^u \mathcal{R}_{lm}(\alpha \cdot z) \epsilon_{mnp} \bar{\chi}_n \gamma_0 \chi_p \right], \quad (3.7)$$

where χ_k is two-component Majorana fermion field

$$\chi_k = \begin{pmatrix} \chi_{+,k} \\ \chi_{-,k} \end{pmatrix} \quad (k = 1, 2, 3) \quad , \quad (3.8)$$

the sign + (-) corresponds to the right (left) movers and $\bar{\chi} = \chi^T \gamma_0$. γ_μ ($\mu = 0, 1$) are chosen as $\gamma_0 = \sigma_x$, $\gamma_1 = i\sigma_y$. The advantage of this model is that the field-shifted gaps agree better with neutron scattering experiments than those of the bosonic model of Eq. (3.5).

B. Isotropic Susceptibility: uniform and staggered

In this subsection, we will forget about the DM interaction and crystal field terms, and discuss the uniform and staggered susceptibilities of isotropic Heisenberg spin-1 chain. In the isotropic case, when an external uniform magnetic field is applied to the system, we assume that the uniform g -tensor is also isotropic. We set $g\mu_B = 1$ in this subsection only.

The Hamiltonian for this case is given by

$$H = \sum_j [J \vec{S}_j \cdot \vec{S}_{j+1} - \vec{h} \cdot \vec{S}_j]. \quad (3.9)$$

Assuming the excitations are non-interacting quasi-particles and no gap anisotropy, the uniform zero-field susceptibility per spin is then

$$\chi_u = \frac{1}{T} \langle (S_z)^2 \rangle = \frac{1}{T} \langle (N_+ - N_-)^2 \rangle, \quad (3.10)$$

where N_\pm are total numbers of quasi-particles with $S_z = \pm 1$.

Since N_+ and N_- are equal in the ground state,

$$\chi_u = \frac{2}{T} (\langle N_+^2 \rangle - \langle N_+ \rangle^2). \quad (3.11)$$

Write

$$N_+ = \sum_k N_{+,k}, \quad (3.12)$$

we get

$$\chi_u = \frac{2}{T} \sum_k (\langle N_{+,k}^2 \rangle - \langle N_{+,k} \rangle^2). \quad (3.13)$$

So for boson and fermion distributions, we have different susceptibilities per unit length as follows:

$$\chi_{u,B} = \frac{2}{T} \int \frac{dk}{2\pi} \frac{e^{\sqrt{\Delta^2 + v^2 k^2}/T}}{(e^{\sqrt{\Delta^2 + v^2 k^2}/T} - 1)^2}, \quad (3.14)$$

$$\chi_{u,F} = \frac{2}{T} \int \frac{dk}{2\pi} \frac{e^{\sqrt{\Delta^2 + v^2 k^2}/T}}{(e^{\sqrt{\Delta^2 + v^2 k^2}/T} + 1)^2}, \quad (3.15)$$

where the gap is $0.4107J$ ^{18,19,20} and the velocity is $2.5J$.²⁰

We plot isotropic boson, fermion, Heisenberg spin-1 chain (transfer-matrix renormalization-group method)²¹, and non-linear σ -model results²² in Fig. 2. We see boson model result is consistent with Heisenberg spin-1 chain result below around $0.2J$, fermion model below roughly $0.5J$, non-linear sigma model result is the best, below roughly $1.5J$.

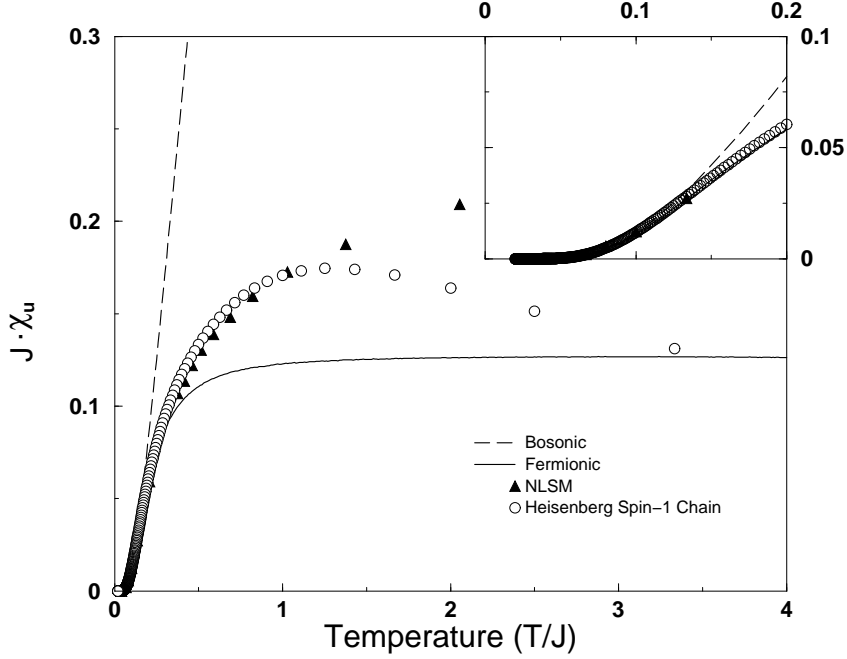


FIG. 2: Comparison of isotropic uniform susceptibilities of different models.

When a staggered magnetic field is applied to the system, the Hamiltonian is

$$H = \sum_j [J \vec{S}_j \cdot \vec{S}_{j+1} - (-1)^j \vec{h} \cdot \vec{S}_j]. \quad (3.16)$$

For the free boson case, the staggered susceptibility is

$$J \cdot \chi_{s,B} = \frac{\rho^2(v/J)}{(\Delta/J)^2} = 14.8\rho^2, \quad (3.17)$$

where ρ is the wave function renormalization of bosonic field. We choose $\rho = 1.11$ to fit the low temperature results of Heisenberg spin-1 chain (TMRG).²¹ They are plotted in Fig. 3. We see they are consistent up to around $0.1J$. We also notice this ρ is consistent with the average value got from the numerical simulations of equal-time correlation function¹³ (in Ref. 13, $g_i = \rho_i^2$):

$$\bar{\rho} = \frac{1}{3}(\rho_x + \rho_y + \rho_z) = 1.12. \quad (3.18)$$

C. Susceptibility of GL Model: uniform and staggered

Susceptibility data has been published for an applied field along the crystallographic a , b or c axis, which is anisotropic. We assume that what is measured is $\partial^2 F / \partial h_a^2|_0$ etc. where F is the free energy and h_a the field

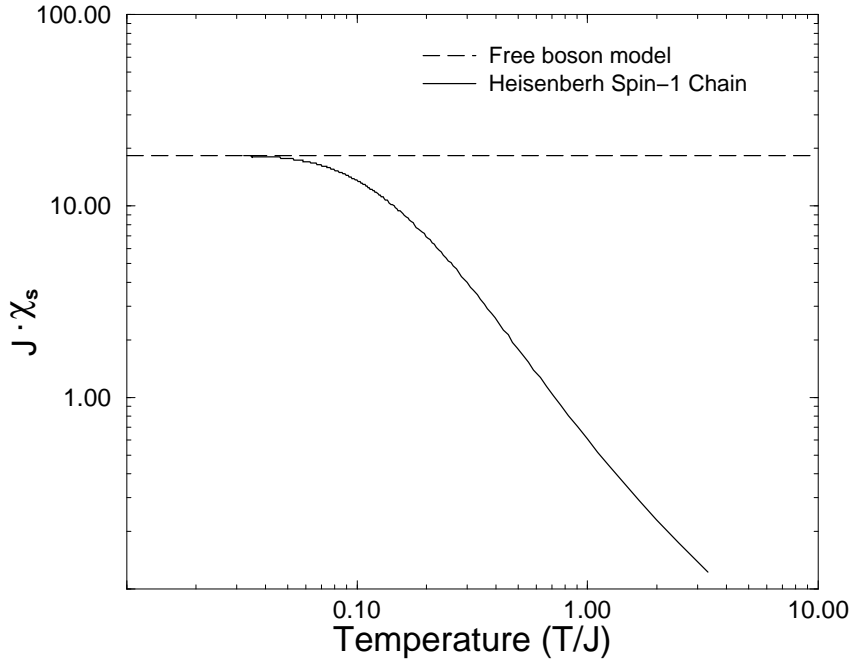


FIG. 3: Comparison of isotropic staggered susceptibilities of different models.

component in the a -direction. From Eqs. (2.25) and (2.24) we get in the (x, y, z) co-ordinate system:

$$\begin{aligned} \chi^{ik} = \frac{1}{L} \frac{\partial^2 F}{\partial h_i \partial h_k} = & \mu_B^2 \sum_{lm} [\mathbf{g}_{il}^u \mathbf{g}_{km}^u \left(\frac{1}{L} \sum_{j_1 j_2, np} \int_0^\beta d\tau \mathcal{R}_{ln}(\alpha \cdot j_1) \mathcal{R}_{mp}(\alpha \cdot j_2) \langle S_{j_1}^n(\tau) S_{j_2}^p(0) \rangle \right) \\ & + \mathbf{A}_{li} \mathbf{A}_{mk} \left(\frac{1}{L} \sum_{j_1 j_2, np} (-1)^{j_1 - j_2} \int_0^\beta d\tau \mathcal{R}_{ln}(\alpha \cdot j_1) \mathcal{R}_{mp}(\alpha \cdot j_2) \langle S_{j_1}^n(\tau) S_{j_2}^p(0) \rangle \right)]. \end{aligned} \quad (3.19)$$

Defining the reduced susceptibility $\bar{\chi}^{ik}(q)$ at arbitrary momentum q:

$$\bar{\chi}^{ik}(q) = \frac{1}{L} \sum_{j_1 j_2} \int_0^\beta d\tau e^{q(j_1 - j_2)} \langle S_{j_1}^i(\tau) S_{j_2}^k(0) \rangle, \quad (3.20)$$

then plugging the explicit form of \mathcal{R} matrix into Eq. (3.19) and use the translation invariance of spin correlation function, χ^{ik} can be written as

$$\chi^{ik} = \mu_B^2 \sum_l \left\{ \mathbf{g}_{il}^u \mathbf{g}_{kl}^u \left[\frac{1 - \delta_{l,z}}{2} \bar{\chi}^{ll}(\alpha) + \delta_{l,z} \bar{\chi}^{ll}(0) \right] + \mathbf{A}_{li} \mathbf{A}_{lk} \left[\frac{1 - \delta_{l,z}}{2} \bar{\chi}^{ll}(\pi + \alpha) + \delta_{l,z} \bar{\chi}^{ll}(\pi) \right] \right\}. \quad (3.21)$$

We expect $\bar{\chi}^{ik}(0)$ to become small at low T .²³ This follows from the fact that it must vanish exponentially in the limit where rotational symmetry around the z -axis is exact. In this case we expect that the groundstate has $S_T^z = 0$ and that there is a finite gap, $\Delta_x = \Delta_y$ to the lowest state of non-zero S_T^z . Thus, at low T , $\bar{\chi}^{zz}(0) \propto e^{-\Delta_x/T}$. The fact that in NENP, $\Delta_x \approx \Delta_y$ suggests that this symmetry is broken only by a small amount. This small symmetry breaking is presumably due to the E^x term in Eq. (1.1) and the DM interaction. As pointed out in Ref. 23, the E^x -term leads to a splitting of the gaps of first order in E^x but a $T = 0$ uniform susceptibility of second order in E^x . This suggests that $\bar{\chi}^{zz}(0)/\bar{\chi}^{xx}(0)$ should be of order $(2/15)^2 = .018$. This estimate was confirmed by an explicit calculation using the Ginzburg-Landau field theory, reviewed above. On the other hand, the experiment obtained a value for this ratio of about .3. While it is possible that this just reflects errors in this rough estimate and in the detailed mean field calculation²³ which confirmed it, it seems more likely that another explanation is required. The explanation could reside in impurity effects or difficulties in separating the spin susceptibility from the diamagnetic contribution. However, later experiments²⁴ at lower T suggest that the impurity contribution doesn't set in until considerably lower T and that the data over the temperature range $T > 1.7K$ may be dominated by the signal from

the pure system. Thus we are led to consider the possibility that this discrepancy may be intrinsic. In this case, the obvious candidate is to include the staggered and uniform DM contributions and the staggered g -tensor at low T . But at high T , both $\bar{\chi}^{ik}(0)$ and $\bar{\chi}^{ik}(\pi)$ go to $2\delta^{ik}/(3T)$. So the staggered contribution to the susceptibility is suppressed by the small factors of A^2 and can be dropped. (Since the staggered g -tensor is proportional to the difference of g -tensor ($g_\xi - g_\zeta$), one may think dropping these terms will eventually affect the staggered g -tensor much. We actually did the calculation by keeping these terms and found the result changes very little.) We also expect the relatively small crystal field Hamiltonian itself to become unimportant at high T . In this limit we have:

$$\chi^{ii} = \frac{\partial^2 F}{\partial h_i^2} = \mu_B^2 \sum_k g_{ik}^u g_{ik}^u \bar{\chi}, \quad (3.22)$$

where $\bar{\chi} \rightarrow 2/(3T)$ at large T . Using the chain rule, the experimental measurements of susceptibility data in the crystallographic co-ordinate system at high T thus give us, approximately, the following results for the g -tensor in the (x, y, z) co-ordinate system:

$$\begin{aligned} g_x^2 \cos^2 \phi + g_y^2 \sin^2 \phi &= (2.23)^2 \\ g_x^2 \sin^2 \phi + g_y^2 \cos^2 \phi &= (2.21)^2 \\ g_z^2 &= (2.15)^2. \end{aligned} \quad (3.23)$$

Setting $\theta = 10^\circ$, $\phi = 58^\circ$, we have from Eq. (2.10)

$$g_\xi = 2.20, \quad g_\eta = 2.24, \quad g_\zeta = 2.15. \quad (3.24)$$

Thus the uniform and staggered g -tensor in the (x, y, z) coordinate system are, from Eqs. (2.10) and (2.11):

$$\mathbf{g}^u = \begin{pmatrix} 2.20 & 0 & 0 \\ 0 & 2.24 & 0 \\ 0 & 0 & 2.15 \end{pmatrix}, \quad (3.25)$$

$$\mathbf{g}^s = \begin{pmatrix} 0 & 0 & 0.008 \\ 0 & 0 & 0 \\ 0.008 & 0 & 0 \end{pmatrix}, \quad (3.26)$$

and matrix \mathbf{A} can be derived from Eq. (2.24).

For the GL model, from Eq. (3.5) we can see there appear two extra terms when a magnetic field is applied to the system:

$$\delta H = - \int dz \mu_B \left[\sum_{iklmn} h_i \mathbf{g}_{ik}^u \mathcal{R}_{kl}(\alpha \cdot z) \epsilon_{lmn} \phi_m \Pi_n + \sum_{ik} h_i^s \mathcal{R}_{ik}(\alpha \cdot z) \rho_k \phi_k \right]. \quad (3.27)$$

Now we use the free field approximation ($\lambda=0$) to calculate the susceptibilities of the spin chain. Expanding ϕ_i and Π_i ($i=x, y, z$) in terms of annihilation and creation operators:

$$\phi_i = \sum_k \sqrt{\frac{v_i}{2L\omega_{ik}}} \{ \exp[-i(\omega_{ik}t - kx)] a_{ik} + h.c. \}, \quad (3.28)$$

$$\Pi_i = \sum_k \sqrt{\frac{1}{2v_i L\omega_{ik}}} (-i\omega_{ik}) \{ \exp[-i(\omega_{ik}t - kx)] a_{ik} - h.c. \}, \quad (3.29)$$

where L is the number of spins and

$$\omega_{ik}^2 = \Delta_i^2 + v^2 k^2. \quad (3.30)$$

If there is no external field, the Hamiltonian becomes

$$H_0 = \sum_{ik} \omega_{ik} (a_{ik}^+ a_{ik} + \frac{1}{2}). \quad (3.31)$$

Looking at δH as a small term, we use first order perturbation theory for eigenstate $|n\rangle$, i.e,

$$|n\rangle \rightarrow |n\rangle - \sum_m \frac{|m\rangle \langle m| \delta H |n\rangle}{E_m - E_n},$$

we have the finite-T formula for susceptibility

$$\chi = \frac{2}{Z} \sum_{n,m} \frac{e^{-\beta E_n} |\langle n | (\delta H/h) | m \rangle|^2}{E_m - E_n}. \quad (3.32)$$

Define reduced uniform and staggered susceptibilities $\bar{\chi}_u$, $\bar{\chi}_s$ at momentum q ($q \ll \pi$) as:

$$\begin{aligned} \bar{\chi}_u^{ik}(q) &= \frac{1}{L} \sum_{j_1 j_2} \int_0^\beta d\tau e^{q(j_1 - j_2)} \langle S_{j_1}^i(\tau) S_{j_2}^k(0) \rangle \\ \bar{\chi}_s^{ik}(q) &= \frac{1}{L} \sum_{j_1 j_2} \int_0^\beta d\tau e^{(\pi+q)(j_1 - j_2)} \langle S_{j_1}^i(\tau) S_{j_2}^k(0) \rangle. \end{aligned} \quad (3.33)$$

From Eq. (3.32) we can calculate them in the GL model as follows:

$$\bar{\chi}_u^{ii}(q) = \frac{1}{2} \int \left(\frac{dk}{2\pi} \right) \frac{1}{\omega_l \omega_m} \left[(1 + n_l + n'_m) \frac{(\omega_l - \omega'_m)^2}{\omega_l + \omega'_m} + (n_l - n'_m) \frac{(\omega_l + \omega'_m)^2}{\omega'_m - \omega_l} \right] \quad (i \neq l \neq m) \quad (3.34)$$

and

$$\bar{\chi}_s^{ii}(q) = \frac{\rho_i^2 v}{\Delta_i^2 + v^2 q^2}. \quad (3.35)$$

In Eq. (3.34), n_{ik} is the bosonic occupation number

$$n_{ik} = \frac{1}{[\exp(\omega_{ik}/T) - 1]}. \quad (3.36)$$

and

$$k' = -k - q, \quad \omega_i = \omega_{ik}, \quad n_i = n_{ik}, \quad \omega'_i = \omega_{ik'}, \quad n'_i = n_{ik'}. \quad (3.37)$$

When the magnetic field is applied along b-axis, the uniform DM interaction will shift the staggered susceptibility by momentum α , but will have no effect on uniform susceptibility. So from Eq. (3.19), the susceptibility along b-axis ($\vec{h} = h\hat{b}$) can be written as

$$\chi^b = (g_z \mu_B)^2 \bar{\chi}_u^{zz}(0) + \frac{1}{2} [(\mathbf{A}_{13} \mu_B)^2 + (\mathbf{A}_{23} \mu_B)^2] [\bar{\chi}_s^{xx}(\alpha) + \bar{\chi}_s^{yy}(\alpha)]. \quad (3.38)$$

Similarly, we can calculate the susceptibility along the a-axis ($\vec{h} = h\hat{a} = h[(\cos 58^\circ)\hat{x} - (\sin 58^\circ)\hat{y}]$). Now the only effect of uniform DM interaction is shifting the uniform susceptibility by momentum α , so we have

$$\chi^a = \frac{1}{2} [(g_x \mu_B \cos 58^\circ)^2 + g_y \mu_B \sin 58^\circ)^2] [\bar{\chi}_u^{xx}(\alpha) + \bar{\chi}_u^{yy}(\alpha)] + \mu_B^2 (\mathbf{A}_{31} \cos 58^\circ - \mathbf{A}_{32} \sin 58^\circ)^2 \bar{\chi}_s^{zz}(0) \quad (3.39)$$

Up to now, we have ignored the velocity differences. The k -integral converges at $k \rightarrow \infty$ so that it is not necessary to introduce an ultra-violet cut-off. Of course a physical cut-off (the lattice spacing) exists in the spin chain but, in the approximation $\Delta \ll J$, including this effect makes only small corrections. On the other hand, taking into account the velocity differences (according to Ref.13, $v_x = v_y = 121K$, $v_z = 114K$), the integrals diverge logarithmically at large k . This implies stronger dependence on the details of the dispersion relation at larger k and the ultra-violet cut-off. However, for the small velocity difference in NENP, we find the susceptibility has very weak cut-off dependence. Changing the cut-off from π to 100π only changes χ^a by about 1%. We just simply ignore this velocity difference.

The staggered and uniform DM vectors are free parameters which can be chosen arbitrarily. We take

$$\frac{D_x}{2J} = -0.008, \quad \frac{D_y}{2J} = -0.02, \quad \frac{D_z}{2J} = 0.04 \quad (3.40)$$

to fit the experimental data. We plot GL model results and experimental data in Fig. 4. The agreement is quite good at low T where the field theory approximations are expected to work.

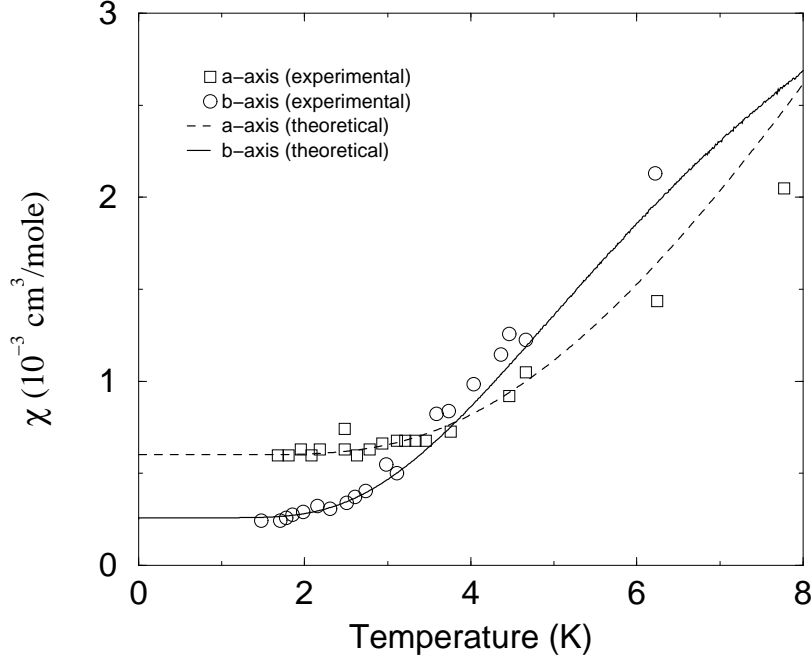


FIG. 4: Measured susceptibility vs the GL model prediction.

D. Susceptibility of Fermion Model: uniform and staggered

For the fermion model, from Eq. (3.7) an extra term appears when a uniform effective field is applied to the system:

$$\delta H = - \int dz \left[\mu_B \sum_{klmnp} i h_k \mathbf{g}_{kl}^u \mathcal{R}_{lm}(\alpha \cdot z) \epsilon_{mnp} \bar{\chi}_n \gamma_0 \chi_p \right]. \quad (3.41)$$

We can also use Eq. (3.32) to compute the finite-T uniform susceptibility of this model. Let us set $D_z = 0$ first, i.e., no uniform DM interaction. Then \mathcal{R} will be identity matrix. We can easily get

$$\chi_F^b = (g_z \mu_B)^2 \bar{\chi}_{u,F}^{zz}(0) \quad (3.42)$$

where in fermion model

$$\bar{\chi}_{u,F}^{ii}(q) = \int \left(\frac{dk}{2\pi} \right) \frac{1}{\omega_l \omega'_m} \left[(1 - n_{l,F} - n'_{m,F}) \frac{\omega_l \omega'_m - |k| \cdot |k'| - \Delta_l \Delta_m}{\omega_l + \omega'_m} + (n_{l,F} - n'_{m,F}) \frac{\omega_l \omega'_m + |k| \cdot |k'| + \Delta_l \Delta_m}{\omega'_m - \omega_l} \right] \quad (i \neq l \neq m). \quad (3.43)$$

Here $n_{i,F}$ is the fermionic occupation number

$$n_{ik,F} = \frac{1}{[exp(\omega_{ik}/T) + 1]}. \quad (3.44)$$

and

$$k' = -k - q, \quad \omega'_i = \omega_{ik'}, \quad n_{i,F} = n_{ik,F}, \quad n'_{i,F} = n_{ik',F}. \quad (3.45)$$

Similarly,

$$\chi_F^a = (g_x \mu_B \cos 58^\circ)^2 \bar{\chi}_{u,F}^{xx}(0) + (g_y \mu_B \sin 58^\circ)^2 \bar{\chi}_{u,F}^{yy}(0). \quad (3.46)$$

The comparison of the uniform susceptibility of bosonic GL model ($D_z = 0$) and that of fermion model ($D_z = 0$) is shown in Fig. 5. The fermion model results are qualitatively similar to the bosonic results for the uniform susceptibility although the $T = 0$ value for χ^a is smaller by about a factor of 50% in the fermionic model. This makes the agreement with the experimental data considerably worse before inclusion of staggered g -tensor and DM interaction.

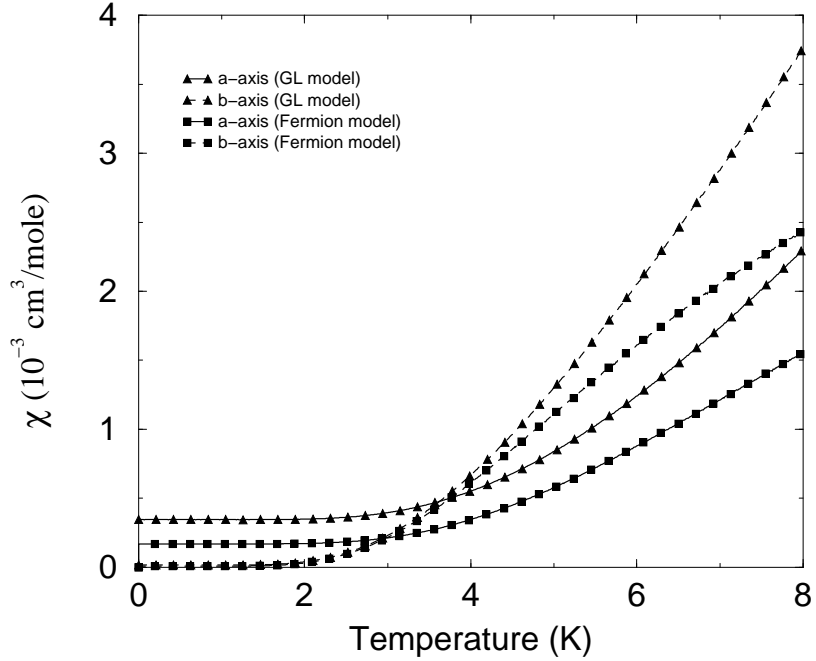


FIG. 5: The comparison of the uniform susceptibility of GL model ($D_z = 0$) and that of fermion model ($D_z = 0$).

Similar to the GL model, we can also include uniform DM interaction into susceptibility calculation. But as we discussed in Sec. IIIA, we don't know how to treat the staggered effective field. If we include uniform DM interaction and simply take the staggered contribution of GL model as that of fermionic model, the total susceptibilities can be calculated and are plotted in Fig. 6. The DM vectors are chosen as

$$\frac{D_x}{2J} = -0.005, \quad \frac{D_y}{2J} = -0.03, \quad \frac{D_z}{2J} = 0.07 \quad (3.47)$$

to fit the experimental data. The agreement is roughly as good as GL model.

IV. DISCUSSION OF OTHER EXPERIMENTAL DATA AND OTHER THEORETICAL APPROACHES

Other experimental anomalies requiring staggered g -tensor and DM interaction for their explanation occur in the Knight shift and field-dependent gaps. Ignoring these small perturbations, the fermionic model is fairly successful at explaining the field-dependent gaps.⁹ The GL model is accurate at low fields but captures only the qualitative features at higher fields where the Zeeman energy is of order the gap.² We find that including the staggered g -tensor and staggered DM interaction does not significantly improve the agreement in the case of the GL model. Including the effect of the uniform DM interaction on the field dependent gaps is a fairly difficult problem even in the GL model approximation since it requires a non-linear treatment of a slowly rotating field, and we do not attempt it here. As remarked above there appears to be no simple way of including the staggered field in the fermion model, thus precluding a calculation of its effects on field-dependent gaps in that model. The field-dependent Knight shift,⁴ presents similar calculational difficulties using GL or fermion model.

There is another low-energy effective field theory model that has been applied to NENP. This model was proposed by Mitra and Halperin.⁵ The Hamiltonian is the following

$$H = \int dz \left\{ \sum_i \left[\frac{v}{2} \Pi_i^2 + \frac{v}{2} \left(\frac{\partial \phi_i}{\partial z} \right)^2 + \frac{\Delta_i^2}{2v} \phi_i^2 \right] - \mu_B \sum_{iklm} h_i \mathbf{g}_{ik}^u \epsilon_{klm} \sqrt{\frac{\Delta_l}{\Delta_m}} \phi_l \Pi_m - \mu_B \sum_i h_i^s \rho_i \phi_i + \lambda \vec{\phi}^4 \right\}. \quad (4.1)$$

In this case we also ignore the small velocity difference which can be shown to have a negligible effect, as in the GL model. This model differs from the standard GL theory of Eq. (3.5) by the factors of $\sqrt{\frac{\Delta_l}{\Delta_m}}$ in the coupling to the magnetic field. These factors were introduced in Ref. (5), in order to obtain field dependent gaps which are the essentially the same as in the fermionic model and hence agree much better with experiment.

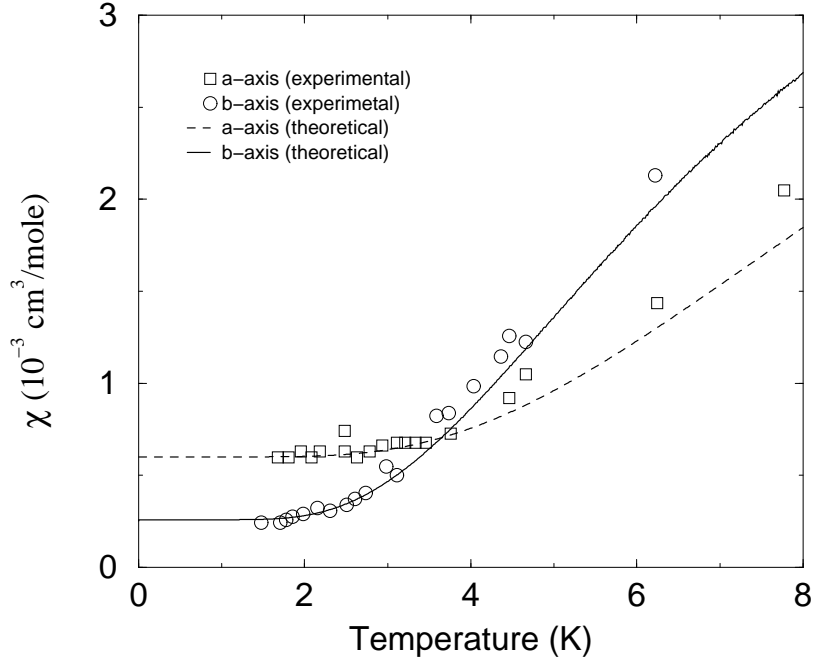


FIG. 6: Measured susceptibility vs the fermion model prediction.

In mean field approximation, the uniform susceptibility is:

$$\chi^b = \frac{1}{2}(g_z\mu_B)^2 \int \left(\frac{dk}{2\pi} \right) \frac{1}{\omega_x \omega_y} \left[(1 + n_x + n_y) \frac{\left(\omega_x \sqrt{\frac{\Delta_y}{\Delta_x}} - \omega_y \sqrt{\frac{\Delta_x}{\Delta_y}} \right)^2}{\omega_x + \omega_y} + (n_x - n_y) \frac{\left(\omega_x \sqrt{\frac{\Delta_y}{\Delta_x}} + \omega_y \sqrt{\frac{\Delta_x}{\Delta_y}} \right)^2}{\omega_y - \omega_x} \right] \quad (4.2)$$

and similarly for χ^a . Note that the k -integral does not converge in the ultraviolet, even ignoring velocity differences, since the integrand behaves as $(\sqrt{\frac{\Delta_y}{\Delta_x}} - \sqrt{\frac{\Delta_x}{\Delta_y}})^2/v|k|$ at large k . Thus the result will be more sensitive to the details of the ultra-violet cut-off than for the other models considered above. Choosing a cut-off, $|k| < \pi$, and ignoring the staggered field gives a value for $\chi^a(T = 0)$ which is about twice as large as that observed experimentally. Including the staggered field raises the theoretical result still higher making the agreement worse. Furthermore, choosing the arbitrary cut-off to be 10π , increases $\chi^a(T = 0)$ by a factor of about 2, also worsening the agreement.

Sieling et al.²⁵, using the Lanczs algorithm and the density matrix renormalization group technique, studied the field-induced gaps, for a field in the z-direction, using a model containing an alternating field and alternating as well as uniform crystal field terms. Independent rotation matrices were assumed for these two types of alternating terms, rather than assuming that both g -tensor and crystal field tensors are diagonal in the (ξ, ζ, η) co-ordinate system, as seems likely. The DM interaction was not included. More numerical work of this type, including the DM interaction (and perhaps also the staggered crystal field terms) and considering the other field direction and the susceptibilities is needed to determine accurate values of the staggered g -tensor and DM interactions.

We would like to thank M. El-Batanouny for asking a question which prompted this investigation and for very helpful discussions on crystal symmetry. This research was supported by NSF grant No. DMR 02-03159.

* Electronic address: huanghai@physics.bu.edu

† Electronic address: iaffleck@physics.ubc.ca

¹ L. P. Regnault et al., *Physica* (Amsterdam) 180B, 188 (1992).

² I. Affleck, *Phys. Rev. B* 41, 6697 (1990).

³ W. Lu et al., *Phys. Rev. Lett.* 67, 3716 (1991).

⁴ M. Chiba et al, *Phys. Rev. B* 44, 2838 (1991).

- ⁵ P. Mitra and B. Halperin, Phys. Rev. Lett. 72, 912 (1994).
- ⁶ I. Dzyaloshinskii, J. Phys. Chem. Solids 4, 241 (1958).
- ⁷ T. Moriya, Phys. Rev. 120, 91 (1960).
- ⁸ I. Affleck, Phys. Rev. Lett. 62, 474 (1989); errata: 65, 2477; 65, 2835 (1990).
- ⁹ A. M. Tsvelik, Phys. Rev. B 42, 10499 (1990).
- ¹⁰ A. Meyer et al., Inorg. Chem. 21, 1929 (1982).
- ¹¹ M. Oshikawa and I. Affleck, Phys. Rev. Lett. 79, 2883 (1997).
- ¹² I. Affleck and M. Oshikawa, Phys. Rev. B 60, 1038 (1999).
- ¹³ E. Sorensen and I. Affleck, Phys. Rev. B 49, 13235 (1994).
- ¹⁴ O. Golinelli et al., Phys. Rev. B 45, 9798 (1992).
- ¹⁵ I. Affleck, in Fields, Strings and Critical Phenomena, Proceedings of the Les Houches Summer School of Theoretical Physics, 1988, edited by E. Brézin and J. Zinn-Justin (Elsevier, New York, 1990), session XLIX.
- ¹⁶ E. Fradkin, Field Theories of Condensed Matter Systems (Addison-Wesley, Redwood City, CA, 1991).
- ¹⁷ I. Affleck, Phys. Rev. B 43, 3215 (1991).
- ¹⁸ S. R. White, Phys. Rev. Lett. 69, 2863 (1992).
- ¹⁹ S. R. White and D. A. Huse, Phys. Rev. B 48, 3844 (1993).
- ²⁰ E. Sorensen and I. Affleck, Phys. Rev. Lett. 71, 1633 (1993).
- ²¹ T. Xiang, Phys. Rev. B 58, 9142 (1998).
- ²² R. M. Konik, cond-mat/0105284.
- ²³ J.P. Renard et al., Europhys. Lett. 3, 945 (1987).
- ²⁴ O. Avenel et al., Phys. Rev. B 46, 8655 (1992).
- ²⁵ M. Sieling et al., Phys. Rev. B 61, 88 (2000).